Silicon Phosphorus Nitride, the First Ternary Compound in the Silicon–Phosphorus–Nitrogen System

H.-P. Baldus*

Bayer AG, ZF-FAF, D-5090 Leverkusen, Germany

W. Schnick[†] and J. Lücke

*Institut für Anorganische Chemie der Universität Bonn,
Gerhard-Domagk-Str. 1, D-5300 Bonn, Germany*

U. Wannagat and G. Bogedain

*Institut für Anorganische und Analytische Chemie der Technischen Universität,
Hagenring 30, D-3300 Braunschweig, Germany*

The novel compound $SiPN_3$ has been prepared by reacting hexachloro-*N*-silylphosphinimine Cl_3Si—N=PCl_3 with liquid ammonia at $-78\,°C$ followed by subsequent removal of the ammonium chloride byproduct and annealing of the resulting polymeric imide at 800 °C for 12 h. The compound has been characterized by elemental analysis and ^{29}Si and ^{31}P MAS-NMR, as well as X-ray powder diffraction methods. The powder data suggest a defect Wurtzite type structure which is closely related to the structures of Si_2N_2O and Si_2N_2NH. (Rietveld analysis data: space group $Cmc2_1$, $Z = 4$, $a = 902.4(4)$ pm, $b = 527.5(2)$ pm, $c = 469.8(2)$ pm; 44 reflections observed; scan range $10° < 2\vartheta < 81°$; germanium monochromator, Cu $K\alpha_1$, $R(wp) = 0.047$, $R(I,h,k,l) = 0.071$.) At 920 °C $SiPN_3$ decomposes into Si_3N_4, P_4, and N_2. The Si_3N_4 obtained on pyrolysis of $SiPN_3$ consists of a pure α-phase and has an extremely low oxygen content.

Introduction

Recently, nitride ceramic materials have gained increased interest owing to their excellent mechanical properties, which are often superior to those of oxide ceramics. In particular their high bending strength, excellent thermal shock resistance, and high hardness makes them attractive engineering materials. Up to now only the binary nitrides of the light elements boron, aluminum, and silicon have been considered for these applications and therefore have been extensively studied.[1–3]

For reasons of analogy the light main-group-element phosphorus should in principle be suitable too for preparation of binary or ternary solid-state nitrides. However, a systematic synthetic approach to this class of compounds was made impossible for a long time by the unavailability of pure, single-phase, defined, and crystalline binary P_3N_5. Recently, Schnick et al. have developed a new synthetic route for this compound.[4] They have started a large-scale investigation on syntheses, characterization, and structure determination of binary phosphorus nitride (P_3N_5) as well as its ternary and quaternary compounds in combination with electropositive elements (e.g., hydrogen and alkali and alkaline-earth metals) using various techniques (single-crystal and powder XRD, ED, HRTEM, EXAFS, IR, ^{15}N and ^{31}P MAS-NMR, impedance spectroscopy, and thermal methods).[4–10] Structural investigations revealed PN_4

tetrahedra to be typical building units of phosphorus nitrides. These units may be interconnected via common vertices to exhibit varying degrees of condensation. In analogy to structural features of well-known phosphates and silicates isosteric P–N partial structures are formed: simple PN_4^{7-} anions have been found in Li_7PN_4,[5] cyclotriphosphate, or silicate-type $P_3N_9^{12-}$ rings occur in $Li_{12}P_3N_9$,[11] and a $P_4N_{10}^{10-}$ cage analogously to molecular phosphorus(V) oxide (P_4O_{10}) has been recently found in $Li_{10}P_4N_{10}$.[7] In HPN_2 and $LiPN_2$ three-dimensional networks $^3_\infty[PN_{4/2}^-]$ topologically identical to and isoelectronic with β-crystobalite have been found,[4,8] and infinite chains of corner-sharing PN_4 tetrahedra $^1_\infty[PN_2N_{2/2}^{4-}]$ occur in PN_3.[10] Even sodalite-type PN_2 framework structures have recently been found[10] and have been modified in several ways. To develop new engineering ceramic materials based on phosphorus nitrides, we tried to stabilize the P–N bond which usually breaks at temperatures above 1000 °C by introducing elements like silicon, aluminum, and boron.

Previous attempts to synthesize such novel ternary nitrides by means of solid-state reaction of the corresponding binary nitrides failed owing to the very small self-diffusion coefficients of those compounds and their incongruent melting behavior. Therefore we developed a new concept of preparation for these materials starting

* Address correspondence to this author.
† New address: Laboratorium für Anorganische Chemie der Unversität Bayreuth, D-8580 Bayreuth, Germany.
(1) Mazdiyasni, K. S.; Cooke, M. *J. Am. Chem. Soc.* **1973,** *56,* 628.
(2) Mazdiyasni, K. S.; Ruh, R. *J. Am. Chem. Soc.* **1981,** *64,* 415.
(3) Lee, R.-R. *J. Am. Ceram. SOc.* **1991,** *74,* 2242.
(4) Schnick, W.; Lücke, J. *Z. Anorg. Allg. Chem.* **1992,** *610,* 121.
(5) Schnick, W.; Lücke, J. *J. Solid State Chem.* **1990,** *87,* 101.

(6) Schnick, W.; Lücke, J. *Solid State Ionics* **1990,** *38,* 271.
(7) Schnick, W.; Berger, U. *Angew. Chem., Int. Ed. Engl.* **1991,** *30,* 830.
(8) Schnick, W.; Lücke, J. *Z. Anorg. Allg. Chem.* **1990,** *588,* 19.
(9) Schnick, W.; Lücke, J. *Angew. Chem., Int. Ed. Engl.* **1992,** *31,* 213.
(10) Schnick, W. *Phosphorus Sulfur,* in press.
(11) Fast Powder Diffractometer System, STOE STADI/P, STOE & CIE., Darmstadt, F.R.G., 1988.

846 *Chem. Mater., Vol. 5, No. 6, 1993*

Baldus et al.

from molecular precursors having the stoichiometries and molecular structures desired in the final ceramic material.

After a polymerization step at low temperatures, a polymeric material is obtained exhibiting a homogeneous distribution of the participating elements. Owing to the short diffusion length provided, a homogeneous distribution on a molecular level allows statistical ordering of the different elements at moderate temperatures, resulting in a new multinary phase. Hence, this concept should work even for materials having very small self-diffusion coefficients in the final state.

In the present work the performance of this approach is demonstrated for the synthesis of the novel compound $SiPN_3$.

Experimental Section

General Procedure. All operations were carried out in an inert atmosphere enclosure (MBraun Inert Gas Systems Model MB 150-GII) or in a standard Schlenk line. Infrared spectra were recorded on a Bruker FTIR 113V spectrometer; solids as KBr pellets or as double mulls (Nujol); liquids as capillary films. NMR experiments with liquid compounds were conducted on a Varian XL 200 spectrometer using $CDCl_3$ as solvent and as an internal standard in case of ^1H NMR. ^{29}Si spectra were recorded using TMS as an internal standard whereas 85% aqueous H_3PO_4 was used as an external standard in ^{31}P NMR measurements. Solid-state MAS-NMR spectra of ^{31}P and ^{29}Si nuclei were recorded on a Bruker WM 300 spectrometer. DTA, TG, and mass spectrometric measurements were carried out simultaneously in nitrogen from room temperature to 1600 °C at 5 °C/min with a Netzsch STA 429 thermobalance system.

The elemental analyses were accomplished at the Bayer analytical laboratories. Phosphorus and silicon were determined by ICP-AES using an acid digestion technique in order to dissolve the samples. Oxygen, nitrogen, and carbon analyses were carried out with Ströhlein Instruments ON-mat 822 and CS-mat 625, respectively.

Oxygen and carbon were detected as CO and CO_2, respectively, in an infrared radiation sensor. Nitrogen was detected with a heat conductivity sensor. Metallic impurities were also detected with the aid of ICP-AES technique.

Transmission electron microscopy and scanning electron microscopy (Philips CM 20) equipped with an EDAX system and coupled with an electron beam diffraction facility were employed for morphology examination, crystal-phase detection, and quantitative elemental analysis, as well as electron beam diffraction on microscopic single crystals.

Crystallographic Measurements and Structure Determination. X-ray powder diffraction measurements were performed on a STOE STADI/P transmission powder diffractometer[12] in Debye–Scherrer mode using sealed 0.3-mm capillaries. Diffraction intensities were recorded by a small linear position-sensitive proportional counter (Mini-PSD, STOE)[12] covering a 2ϑ range of 6.7°. A curved germanium monochromator was used to obtain a focused monochromatized Cu $K\alpha_1$ primary beam (λ = 154.056 pm). Thus during an exposure time of 12 h in a 2ϑ range of 10–81°, sufficiently high counting rates and a total number of 44 reflections were obtained. For the structure refinement step intensities were used with an angular resolution of about 0.06°. All calculations were carried out using the STOE STADI/P software package.[11]

Materials. Ammonia 5.0 (Messer Griesheim, O_2 < 5 ppm, H_2O < 15 ppm) was used as received; $SiCl_4$ and hexamethyldisilazane (Bayer AG) were redistilled before use. PCl_3 (Merck Schuchardt) was used as received. All the solvents were purified and dried by standard procedures before use.

Synthesis of $SiPN_3$. *Synthesis of Cl_3Si—N=PCl_3 (A).* The synthesis of Cl_3Si—N=PCl_3 is performed according to a procedure described by Filonenko et al.[12,13]

Synthesis of $SiPN_3$ (B). A 4000-mL four-necked round-bottomed flask, equipped with a dropping funnel, pressure filter funnel, gas inlet, pressure release valve, and a mechanical stirrer is loaded with ca. 2.5-L anhydrous ammonia at –70 °C. Compound A (472 g, 1.66 mol) dissolved in 500 mL of hexane is added dropwise to the ammonia within 2 h under vigorous stirring. A vigorous reaction occurs during which white fumes evolve and a white solid precipitates. The reaction mixture is stirred for an additional 2 h at –78 °C and then the white precipitate is filtered off in a stream of argon using a pressure filter funnel. After filtration the NH_4Cl produced by the ammonolysis reaction is extracted with liquid NH_3 for 4 days. The remaining white powder is dried under reduced pressure at 150 °C in order to remove the rest of absorbed ammonia. A white powder is obtained with the following elemental analysis: Si 19.2% (18.4%); P 22.0% (20.4%); N 50.5% (55.3%); H 5.9% (5.9%); Cl 0.1%, O 1.3%. The values given in parentheses are calculated for the formula $SiPN(NH)(NH2)_4$. The deviation between the observed and calculated values regarding the nitrogen content is most probably due to moisture contamination and subsequent loss of ammonia during handling of this very moisture-sensitive material.

For pyrolysis, samples of the as-received powder are placed into a boron nitride boat and inserted into a quartz tube equipped with two ground glass joints. Before use the quartz tube has to be heated to 400 °C in vacuum in order to remove the adsorbed water from the walls.

All loading operations are performed in a N_2-filled glovebox, using N_2 which is purified in-line over molecular sieves, P_2O_5 and Cr(II) catalysts in an attempt to minimize O_2 and H_2O contamination (both <0.3 ppm). The powder samples are pyrolyzed in a programmable tube furnace. Initially that quartz tube is flushed with anhydrous NH_3 at room temperature. The powder is heated under flowing anhydrous NH_3 from room temperature to 800 °C with a heating rate of 5 °C/min then held at that temperature for an additional 10–15 h and finally cooled to room temperature over at least 6 h.

The material obtained this way is partially crystalline with a high degree of disorder. Elemental analysis: Si 27.1% (27.7%); P 29.3% (30.7%); N 41.4% (41.6%); H 1.1%; Cl 0.03%; O 0.4%. These data are in accordance with the chemical composition $SiPN_3$ (the calculated values are given in parentheses). The yield obtained corresponds to theoretical value calculated from the initial amounts of silicon and phosphorus, respectively. To get a well-crystallized material the as-received powder is filled in a quartz tube together with a small amount of NH_4Cl as crystallizing agent. The quartz tube is evacuated, sealed and the mixture is annealed at 900 °C for an additional 24 h. The pressure within the tube can be estimated from the amount of NH_4Cl added by employing the ideal gas equation. To avoid risk of explosion, it should not exceed 10 bars. At the end of this procedure NH_4Cl is removed by sublimation in vacuum.

Results and Discussion

Low-Temperature Ammonolysis of Cl_3Si—N=PCl_3 and Characterization of the Resulting Polymer. The starting compound Cl_3Si—N=PCl_3 is obtained in good yield (86%) by a route according to Filonenko and Pinchuk.[13]

The ammonolysis reaction was carried out at –78 °C due to the high excess enthalpy expected for the reaction. To eliminate all chlorine functionalities, the phospinimine was dissolved in hexane and added dropwise to a large excess of liquid ammonia. We suggest a reaction according to eq 1. After the removal of the ammonium chloride by

$$xCl_3Si\text{—}N\text{=}PCl_3 + 12xNH_3 \rightarrow$$
$$\{SiPN(NH)_{3-y}(NH_2)_{2y}\}_x + 6xNH_4Cl \quad (y = 0\text{--}3) \quad (1)$$
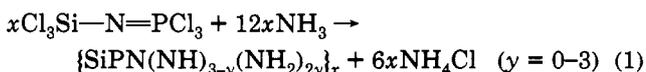
extraction with liquid ammonia a white, amorphous

(12) Filonenko, L. P.; Pinchuk, A. M. *J. Gen. Chem. USSR* **1979**, *49*, 302.

(13) Filonenko, L. P.; Pinchunk, A. M. *J. Gen. Chem. USSR* **1979**, *49*, 348.

Silicon Phosphorus Nitride

Chem. Mater., Vol. 5, No. 6, 1993 847
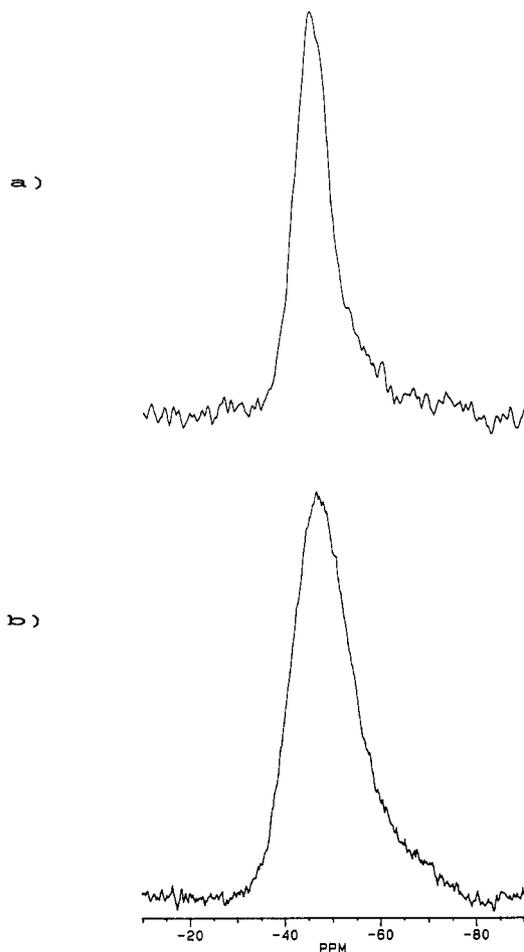
Figure 1. ^{29}Si NMR spectra of silicon phosphorus nitride materials: (a) amorphous polymer; (b) crystalline SiPN$_3$.

Figure 2. ^{31}P NMR spectra of silicon phosphorus nitride materials: (a) amorphous polymer (the badly resolved peaks at -50 ppm are spinning sidebands of the major peaks); (b) crystalline SiPN$_3$.

powder is obtained. The analytical data of this material correspond to the chemical composition SiPN(NH)(NH$_2$)$_4$.

Due to the amorphous structure of the resulting phosphorus silicon imide–amide, ^{29}Si solid-state MAS-NMR spectra show a broad signal at ca. -43 ppm (Figure 1a), indicating that silicon is tetrahedrally coordinated by nitrogen atoms.[14] The polymeric compound exhibits two ^{31}P NMR signals at 25.3 and 14.7 ppm (Figure 2a). Comparison of these data with ^{31}P NMR data of amino-phosphazenes shows that the resonance at 14.7 ppm can be assigned to —N=P(NH$_2$)$_2$—N— moieties.[15] Assuming that an enhanced cross-linking of the P–N– network leads to a high-field shift of the ^{31}P resonances as is observed for phosphorus oxides,[16] we can attribute the signal at 25.3 ppm to —N=P(NH$_2$)$_3$— end groups. The IR spectrum of the polymer (Figure 3a) shows five distinct regions. A band at 3440 cm^{-1} is attributed to the NH stretching vibration. At 2179 cm^{-1} we observe a combination mode of the Si–N and P–N vibrations. The IR absorption signal at 1636 cm^{-1} represents the N–H deformation vibration. The broad band between 1450 and 1200 cm^{-1} can be assigned to the P=N—P asymmetric stretches whereas the signal at 940 cm^{-1} is attributed to the Si–N stretching vibration. The high wavenumber of

the P–N stretching vibration is consistent with an enhanced PN bond order and a bond polarity $^+$P–N$^-$.[17]

Synthesis and Characterization of SiPN$_3$. On heating the preceramic polymer in a flow of ammonia at 800 °C for at least 10 h we obtain partially crystalline SiPN$_3$. Ammonia is the preferred atmosphere since it enhances the crystallinity of the sample. Nearly complete crystallization can be achieved by annealing the polymeric imide at 900 °C for 24 h using ammonium chloride as a mineralizing agent. According to TGA/DTA measurements performed in nitrogen between room temperature and 1600 °C, the conversion of the polymer to the crystalline compound is accompanied by a weight loss of about 28% in the range between 150 and 900 °C (Figure 4a). The pyrolysis gases evolved during this stage consist only of ammonia as revealed by simultaneous mass spectrometric analyses. Therefore we conclude according to eq 2 that this loss of ammonia is owing to further polycondensation until the composition of stoichiometric SiPN$_3$ is achieved.

$$SiPN(NH)(NH_2)_4 \rightarrow SiPN_3 + 3NH_3 \qquad (2)$$

The theoretical weight loss of 26.8% matches closely the observed value which gives further evidence to the above proposed reaction scheme.

(14) Carduner, K. R.; Carter III, R. O.; Milberg, M. E.; Crosby, G. M. *Anal. Chem.* **1987**, *59*, 2794.

(15) Crutchfield, M. M.; Dungan, C. H.; Letcher, J. H.; Mark, V.; Van Wazer, J. R. ^{31}P Nuclear Magnetic Resonance. In *Topics in Phosphorus Chemistry*; John Wiley: New York, 1968; Vol. 5.

(16) Losso, P.; Schnabel, B.; Jäger, C.; Sternberg, U.; Stachel, D.; Smith, D. O. *J. Non-Cryst. Solids* **1992**, *143*, 265.

(17) Wannagat, U.; Burgdorf, D.; Bürger, H.; Pawelke, G. *Z. Natur-forsch.* **1991**, *46b*, 1039.
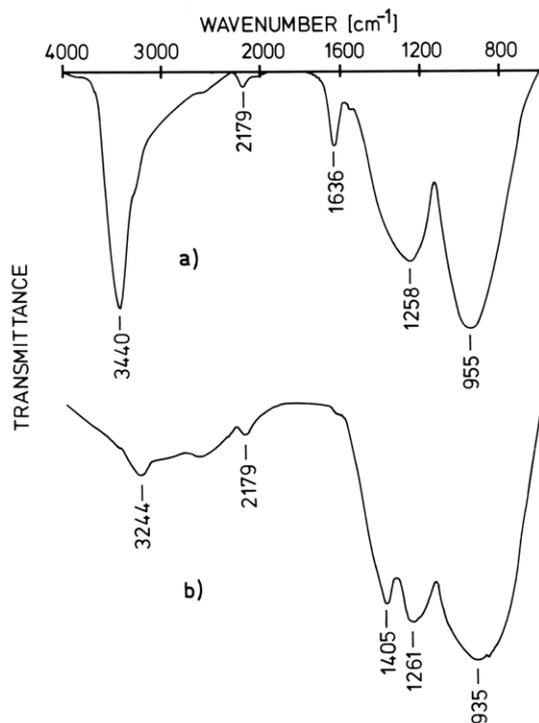
Figure 3. IR spectra of silicon phosphorus nitride materials: (a) amorphous polymer; (b) crystalline $SiPN_3$.
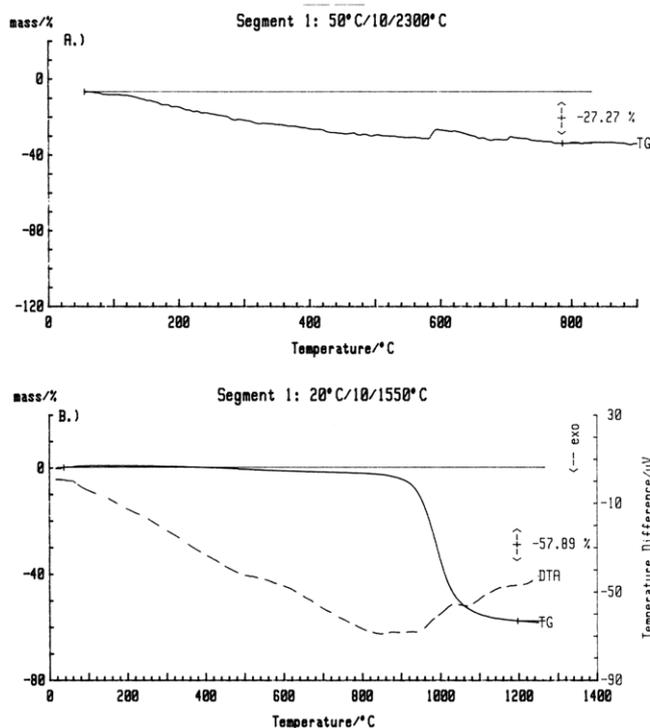
Figure 4. TG/DTA plots of silicon phosphorus nitride materials: (a) TG/DTA curve of the amorphous polymer between room temperature and 900 °C; (b) TG/DTA curve of crystalline $SiPN_3$ between 900 and 1500 °C.

Electron microscopic analyses (TEM/EDAX) on microscopic single crystals show a Si:P ratio of 1:1. SEM micrographs reveal well-defined crystals with a size in the range from 5 to 50 μm (Figure 5). The signal of the ^{29}Si MAS NMR spectrum is observed at −46 ppm (Figure 1b). This value is close to the ^{29}Si NMR signal of silicon nitride[18] and can therefore be attributed to silicon atoms tetrahe-

(18) Carduner, K. R.; Hatfield, G. R. *J. Mater Sci.* **1989**, *24*, 4209.
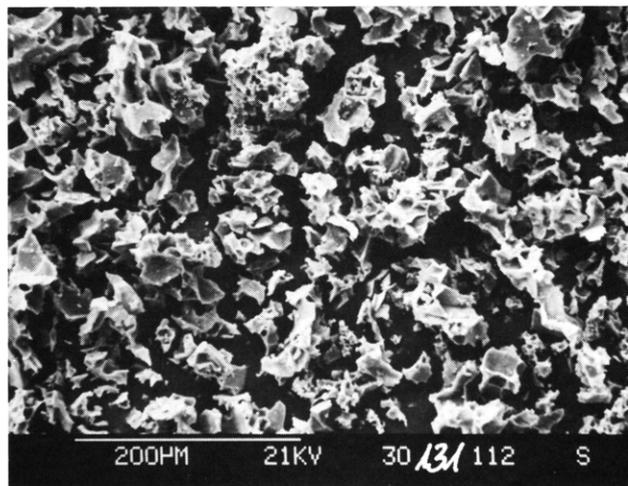
Figure 5. Scanning electron micrograph of microcrystalline $SiPN_3$.

drally coordinated by nitrogen. Compared to the value of the ^{29}Si resonance in the preceramic polymer the observed high-field shift suggests an increased degree of cross linking of the material. The ^{31}P NMR resonance of the crystalline $SiPN_3$ is detected at −12 ppm (Figure 2b).

This value fits well into the series of polymeric P–N compounds such as $LiPN_2$, HP_4N_7, and P_3N_5, containing three-dimensionally connected PN_4 tetrahedra. The ^{31}P NMR resonance is increasingly high-field shifted with increasing degree of cross-linking (^{31}P resonances: $LiPN_2$ (0 ppm), HP_4N_7 (−26 ppm), P_3N_5 (−46 to −65 ppm)).[19] This is in agreement with the crystal structure of the compound described below. The high-field shift of the ^{31}P signal (35 ppm) after the conversion of the material from the polymeric state into the crystalline state is very large compared to the shift of the ^{29}Si signal (3 ppm) which may be due to the very large bandwidth of the ^{31}P resonances. The width of the ^{31}P NMR signal of about 50 ppm may be due to the high degree of disorder in the crystalline state.

Infrared spectra of the crystalline solid (Figure 3b) show three main absorption bands. The weak absorption at 3440 cm^{-1} suggests the presence of residual N–H groups in the solid. The shoulder at 1405 cm^{-1} as well as the bands at 1250 and 937 cm^{-1} can be assigned to the asymmetric P≡N—P and Si—N—Si stretches respectively. The band at 2179 cm^{-1} is again due to a combination of P—N and Si—N stretches. A comparison of the P—N≡P and Si—N—Si IR absorption bands of the amorphous polymer and the crystalline material shows no significant difference, indicating that the bonding situation and the short-range order in the solid in both the amorphous and the crystalline compound are rather similar. The similar width of the respective absorption bands of the amorphous and the crystalline solids is consistent with the assumption that the long-range order in the crystals is strongly disturbed.

Structure Determination. All of the observed X-ray reflections (Table I) could be indexed assuming orthorhombic symmetry and a C-centered Bravais lattice. The unit-cell dimensions of $SiPN_3$ also were confirmed by electron diffraction on microscopic single crystals. Analysis of the observed powder pattern of $SiPN_3$ (Figure 6)

(19) Schnick, W.; Lücke, J. Manuscript in progress.
(20) Peters, D.; Jacobs, H. *J. Less-Common Met.* **1989**, *146*, 241.
(21) Idrestedt, I.; Brosset, C. *Acta Chem. Scand.* **1964**, *18*, 1879.
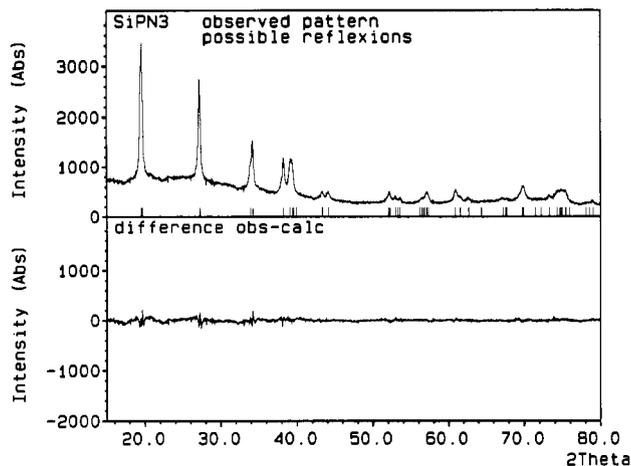
Figure 6. Powder diffraction pattern of SiPN$_3$ showing the observed powder pattern and difference (bottom) pattern.

Figure 7. Crystal structure of SiPN$_3$ (filled circles = P, Si atoms, empty circles = N atoms).

Table I. Observed and Calculated X-ray Reflections of SiPN$_3$ (Cu Kα_1 Radiation, λ = 154.056 pm)

h	k	l	2ϑ	fwhm	I_{obs}	I_{calc}
1	1	0	19.473	0.342	356.63	353.78
2	0	0	19.657	0.325	912.45	857.01
1	1	1	27.247	0.364	887.57	835.13
0	2	0	33.956	0.399	106.61	139.18
3	1	0	34.286	0.401	360.73	362.90
0	0	2	38.281	0.422	353.25	330.54
0	2	1	39.131	0.426	242.32	225.88
3	1	1	39.422	0.428	328.49	294.19
2	2	0	39.540	0.428	0.08	0.07
4	0	0	39.925	0.430	2.14	1.04
1	1	2	43.300	0.448	36.32	38.86
2	0	2	43.389	0.448	44.16	47.71
2	2	1	44.157	0.452	83.69	92.42
0	2	2	52.089	0.494	55.05	52.85
3	1	2	52.322	0.495	92.79	95.78
1	3	0	53.007	0.499	52.82	44.58
4	2	0	53.391	0.501	0.09	0.08
5	1	0	53.621	0.502	56.45	50.95
2	2	2	56.209	0.515	14.37	10.68
4	0	2	56.505	0.517	41.92	36.87
1	3	1	56.773	0.518	10.55	9.81
4	2	1	57.140	0.520	79.28	80.06
5	1	1	57.359	0.521	65.26	71.92
3	3	0	60.977	0.540	151.05	139.24
6	0	0	61.608	0.543	62.21	59.62
1	1	3	62.677	0.549	43.30	47.10
3	3	1	64.443	0.558	6.00	6.94
1	3	2	67.251	0.573	20.80	31.29
4	2	2	67.584	0.574	2.45	3.89
5	1	2	67.783	0.575	10.76	17.59
0	2	3	69.778	0.586	106.61	101.08
3	1	3	69.974	0.587	132.52	129.01
0	4	0	71.467	0.595	15.48	20.92
6	2	0	72.244	0.599	14.68	20.43
2	2	3	73.298	0.604	66.43	69.53
3	3	2	74.327	0.610	110.42	103.13
0	4	1	74.687	0.611	31.34	30.05
6	0	2	74.902	0.613	67.26	64.81
2	4	0	74.955	0.613	37.64	36.31
5	3	0	75.401	0.615	32.97	33.40
6	2	1	75.451	0.615	89.26	91.70
7	1	0	75.909	0.618	0.11	0.17
2	4	1	78.123	0.629	5.48	17.03
5	3	1	78.563	0.632	8.23	9.23
7	1	1	79.064	0.634	42.82	37.02

Table II. Metric Similarities of the Unit Cells of SiPN$_3$, Si$_2$N$_2$NH, and Si$_2$N$_2$O

	SiPN$_3$	Si$_2$N$_2$NH[20]	Si$_2$N$_2$O[21]
a, pm	902.4(4)	919.30(7)	884.3(5)
b, pm	527.5(2)	540.96(4)	547.3(5)
c, pm	469.8(2)	481.90(4)	483.5(5)

Table III. Fractional Coordinates and Isotropic Thermal Parameters ($\times10^4$) with ESDs for SiPN$_3$

atom	site	x	y	z	U(iso)
Si/P	8b	3294(13)	3406(34)	0	95(34)
N1	8b	2859(35)	3753(89)	3556(52)	25(108)
N2	4a	0	2535(75)	4225(109)	25(108)

Table IV. Selected Bond Distances (pm) and Angles (deg) (with ESDs) in SiPN$_3$

P/Si–N2	165.8(20)		
P/Si–N1	168.3(41)	168.9(46)	173.0(25)
P/Si–N1–P/Si	125.8(17)	117.1(23)	115.2(23)
P/Si–N2–P/Si	136.3(29)		

revealed an analogy between the crystal structures of SiPN$_3$ and that of Si$_2$N$_2$NH or Si$_2$N$_2$O (Table II).

On the basis of this analogy the crystal structure of SiPN$_3$ was refined by the use of a modified version of the Rietveld full-profile method.[11] For the structure refinement step intensities in the 2ϑ range 10–81° were used with an angular resolution of about 0.06°. Due to the rather symmetrical peak shape a modified Lorentzian function (Mod 2 Lorentzian) proved to be suitable for representation of the individual reflection profiles. The angular dependence of the peak full-width at half-maximum (fwhm) was described by a proper Tchebychev polynomial. The background intensity line was also refined during the calculation using a Tchebychev polynominal of up to the seventh degree. The integration range used was 6.0 fwhm on both sides of the diffraction line positions. Refinement of the half-width parameters, the zero-point, and the scale factor was performed before the refinement of the positional parameters was started. The refinement of the crystal structure of SiPN$_3$ was started on the basis of the similarity of the powder patterns of SiPN$_3$ and Si$_2$N$_2$O assuming a statistical distribution of Si and P on the silicon sites and with nitrogen on both of the anionic positions (N and O) in Si$_2$N$_2$O. Neither during the Rietveld refinement nor by electron diffraction on small single crystals of SiPN$_3$ any experimental evidence for an ordered distribution of Si and P resulting in a superstructure (lower space-group symmetry or larger unit cell) occurred. The refinement (seven structural and three isotropic thermal parameters refined, 44 reflections observed) converged with final residual factors of $R(p)$ = 0.0327 and R(wp) = 0.0472 for the profile and $R(I,hkl)$ = 0.0710 for the structure. Atomic coordinates of SiPN$_3$ are summarized in Table III, interatomic distances and bonding angles are given in Table IV. Silicon phosphorus nitride SiPN$_3$ exhibits a three-dimensional polymeric network structure of corner sharing PN$_4$ and SiN$_4$ tetrahedra (Figure 7). Analogously to Si$_2$N$_2$O and Si$_2$N$_2$NH the crystal structure derives from a defect Wurtzite-type arrangement. Thus two-dimensional planes of condensed Si$_3$N$_3$ rings occur with half of the silicon atoms being replaced by phosphorus. The puckered six-membered rings show boat conforma-

850 *Chem. Mater., Vol. 5, No. 6, 1993*

Baldus et al.

tion. The silicon and phosphorus atoms seem to be statistically distributed. By means of X-ray powder crystallography a distinction between phosphorus and silicon in $SiPN_3$ was not possible. The infinite layers of condensed $(Si/P)_3N_3$ rings perpendicular to the a axis of the orthorhombic unit cell represent a distorted variant of typical Wurtzite-type layers. Condensation to a three-dimensional network is achieved by the bridging nitrogen atoms (N2), each connecting two Wurtzite-type $(Si/P)_3N_3$ layers in a direction saturating the remaining free valences of phosphorus and silicon, respectively.

Pyrolysis of $SiPN_3$. Heating of the crystalline $SiPN_3$ above 900 °C in the TG/DTA apparatus (Figure 4b) leads to a significant weight loss of about 57.6% in the range 920–1100 °C. In this temperature range the pyrolysis gases contain mainly P_4 and N_2 according to the mass spectrometric data which are detected simultaneously during the TG/DTA experiment which gives strong evidence for a decomposition of $SiPN_3$. The decomposition of the material is also indicated by an endothermic DTA signal at ca. 1000 °C. According to X-ray measurements the 1000 °C material is completely amorphous, indicating the breakdown of the $SiPN_3$ structure in the solid.

On further pyrolysis up tp 1200 °C we observe an exothermic DTA signal at ca. 1100 °C. X-ray analysis of material heated at that temperature show a new diffraction pattern which corresponds to α-Si_3N_4. Thus we can assign the exothermic DTA signal to the crystallization of α-silicon nitride. Elemental analysis data obtained on this material reveal a phosphorus content of only 200 ppm. In summary these data lead to the conclusion that the decomposition of $SiPN_3$ occurs between 900 and 1000 °C leading to an amorphous silicon nitride which finally crystallizes around 1100 °C. The corresponding reaction pathway is described in eq 3. The theoretical weight loss

$$12SiPN_3 \xrightarrow{900–1000\ °C} 4Si_3N_4\ (\text{amorphous}) + 3P_4 + 10N_2$$
$$\xrightarrow{1100\ °C} \alpha\text{-}Si_3N_4 \quad (3)$$
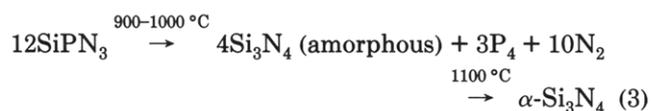
for the decomposition of $SiPN_3$ into Si_3N_4 according to eq 3 amounts to 53.8%. The observed weight loss of 57% is about 3% higher than the theoretical value. This discrepancy may be explained by the loss of residual NH groups and the removal of oxygen from the $SiPN_3$ material during the decomposition. This hypothesis is consistent with the extremely low oxygen content (200–400 ppm) of our silicon nitride material derived from the decomposition of $SiPN_3$. An explanation for this finding is that the gaseous phosphorus released from $SiPN_3$ at temperatures above 900 °C acts as an oxygen getter.

A second interesting feature is the high α-phase content of such a $SiPN_3$-derived material annealed at 1250 °C for 3 h, which is in the range from 98% to 100%. The α-phase content of conventionally synthesized crystalline silicon nitride is normally in the range 80–90%. A further unusual property of our material is the high degree of sintering and Ostwald ripening of the α-Si_3N_4 crystals obtained on annealing at 1250 °C for 3 h (Figure 8). Owing to the low oxygen content of the material, one would expect just the opposite effect, very small crystals with a narrow particle size distribution. A possible reason for this behavior is

$\dashv\ \vdash$
5 µm
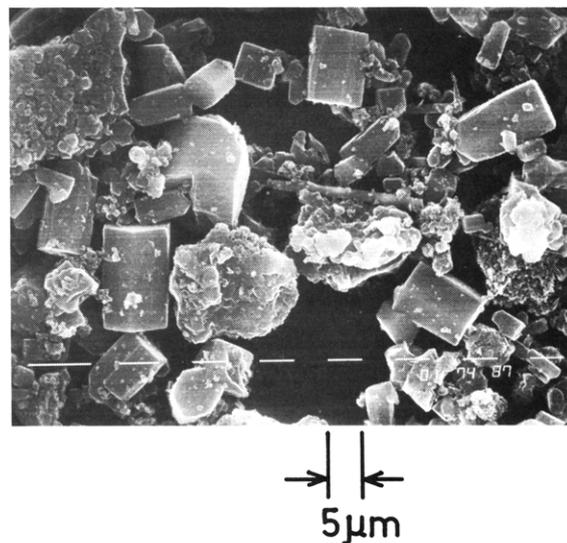
Figure 8. Scanning electron micrograph of α-Si_3N_4 derived from $SiPN_3$ pyrolyzed at 1400 °C for 2 h.

the formation of species with high diffusion coefficients during the breakdown of the $SiPN_3$ structure (including Si–N bond cleavage) between 900 and 1200 °C. These species should cause a highly enhanced solid-state diffusion within the material which may lead to the observed sintering and Ostwald ripening effects.

Conclusions and Outlook

We have synthesized a novel ternary nitride, $SiPN_3$, through tailoring a molecular precursor compound to the elemental stoichiometry of the desired final material. The structure of $SiPN_3$ is isotypic to the structures of Si_2N_2O and Si_2N_2NH. This observation may be rationalized by taking into account that SiO and PN are isoelectronic.[17] Our experiments show that the P–N bond in $SiPN_3$ is not stabilized by the presence of silicon, and hence it is not suitable as a high-temperature ceramic by itself. Nevertheless, it may have some interesting applications in the field of the processing of non-oxide powders. Decomposition of $SiPN_3$ at ca. 1000 °C yields Si_3N_4 and gaseous P_4, which acts as an oxygen getter. Annealing the obtained Si_3N_4 at 1250 °C for 3 h yields pure α-Si_3N_4 which can serve as a crystallizing agent. Therefore, calcination of commercially produced amorphous Si_3N_4 together with small amounts of $SiPN_3$ should lead to crystalline silicon nitride with a low oxygen content and a high amount of the desired α-phase. On the other hand, considering the unexpected sintering effects observed at the crystalline Si_3N_4 powder obtained from pyrolysis of $SiPN_3$, this compound could also serve as a sintering additive for silicon nitride by promoting the solid state diffusion within the ceramic body. Experiments concerning these possible applications of $SiPN_3$ are under way.